文章编号:1006-9941(2025)03-0295-09

Solubility and Thermodynamic Modeling of 3-Nitro-1,2,4-triazole-5-one (NTO) in Different Binary Solvents

GUO Hao-qi, YANG Yu-lin

(*State Key Laboratory of Space Power-Sources, School of Chemistry and Chemical Engineering, Harbin Institute of Technology, Harbin* 150001, *China*)

Abstract: Using a dynamic laser monitoring technique, the solubility of 3-nitro-1,2,4-triazole-5-one (NTO) was investigated in two different binary systems, namely hydroxylamine nitrate (HAN)-water and boric acid (HB)-water ranging from 278.15 K to 318.15 K. The solubility in each system was found to be positively correlated with temperature. Furthermore, solubility data were analyzed using four equations: the modified Apelblat equation, Van't Hoff equation, λh equation and CNIBS/R-K equations, and they provided satisfactory results for both two systems. The average root-mean-square deviation (10^5RMSD) values for these models were less than 13.93. Calculations utilizing the Van't Hoff equation and Gibbs equations facilitated the derivation of apparent thermodynamic properties of NTO dissolution in the two systems, including values for Gibbs free energy, enthalpy and entropy. The $\%\zeta_H$ is larger than $\%\zeta_{TS}$, and all the $\%\zeta_H$ data are ≥58.63%, indicating that the enthalpy make a greater contribution than entropy to the ΔG_{soln}^{Θ}.

Key words: 3-nitro-l,2,4-triazole-5-one (NTO); solubility; thermodynamic models; apparent thermodynamic analysis

CLC number: TJ55; O64 **Document code:** A **DOI:** 10.11943/CJEM2024184

0 Introduction

Hydroxyamine nitrate (HAN)-based electrically controlled solid propellants, relying on their unique electrochemical properties, can achieve multiple starts and thrust adjustments[1], which makes up for the working defect of traditional solid engines that cannot be shut down at any time after ignition. It is expected to meet the military requirement for controllable combustion of solid propellants. However, in the present study, HAN-based electrically controlled solid propellant has the problem of multi-step thermal decomposition and small energy density, which seriously limits its practical application. The energy characteristics of propellants can be improved by adding other energetic substances to the system. 3-Nitro-1,2,4-triazole-5-one(NTO) is a single material explosive with water-soluble, high energy density, and low sensitivity[2]. Compared to hexahydro-1, 3, 5-trinitro-2,4,6-triazine(RDX)[3], octahydro-1,3,5,7-tetranitro-1, 3, 5, 7-tetrazocine (HMX)[4], and hexanitrohexaazaisowurtzitane (CL-20)[5], NTO has the characteristic of only burning without exploding under flame stimulation, as well as its similar thermal decomposition products(NO, CO, CO_2, N_2O and H_2O) to HAN[6], making it more suitable for electrically controlled solid propellant systems. In addition, lone pair electrons on carbonyl oxygen atoms, nitro oxygen atoms, and nitrogen heterocyclic atoms in NTO molecules can form complexes with metal ions, making the propellant system more stable[7]. The performance test of the electrically controlled solid propellant containing NTO shows significant improvements in energy characteristics, with increased burning heat and thermal decomposition temperature, but

Received Date: 2024-07-05; **Revised Date:** 2024-12-25

Published Online: 2024-12-25

Biography: GUO Hao-qi(1994-), male, PhD candidate, mainly engaged in the research of energetic materials and their applications. e-mail:530825119@qq.com

Corresponding author: YANG Yu-lin(1969-), male, professor, mainly engaged in the research of energetic materials and their applications. e-mail:ylyang@hit.edu.cn

引用本文:郭昊琪,杨玉林. 3-硝基-1,2,4-三唑-5-酮(NTO)在不同二元溶剂中的溶解度和热力学模型[J]. 含能材料,2025,33(3):295-303.

GUO Hao-qi, YANG Yu-lin. Solubility and Thermodynamic Modeling of 3-Nitro-1,2,4-triazole-5-one (NTO) in Different Binary Solvents[J]. *Chinese Journal of Energetic Materials(Hanneng Cailiao)*,2025,33(3):295-303.

there are still some problems. For example, the solid NTO dissolves and forms local voids during the heating and solidification process of the propellant, and the excessive addition of NTO leads to uneven solid dispersion. To obtain high-quality propellant samples, it is necessary to determine the solubility of NTO in the propellant system before adding NTO to optimize the performance of electronically controlled solid propellants. The main components of electrically controlled solid propellants, including acidic hydroxylamine nitrate (HAN), boric acid (HB), and water content, directly affect the solubility of NTO in the system. Based on the practical application, propellant formulation and preparation conditions, this study set the concentration gradient of the solution (HAN aqueous solution: 10%−70%, gradient 10%, HB aqueous solution: 1.0%−2.5%, gradient 0.5%), and experimental temperature of 278.15−318.15 K, and the solubility of NTO in HAN-water and HB-water binary solvent systems was obtained using dynamic laser monitoring method. In addition, the optimum model was obtained by comparing the fitting parameters of the solubility model.

In this work, the effects of different HAN and HB contents on the dissolution behavior of NTO in water at the temperature of 278.15−318.15 K and the specific solubility values were clarified. In the subsequent process of improving the performance of propellants, when the propellant formulation and curing temperature change, the solubility of NTO in the propellant system under the current process conditions can be obtained directly through the model calculation. This word is beneficial for the rapid adjustment of propellant formulations, thereby improving work efficiency.

1 Experimental

1.1 Materials

NTO was sourced from Jiangyang Chemical Co., Ltd. with a HPLC (high-performance liquid chromatography) purity of 99.8% (Fig.1), and the molecular structure as presented in Fig.2. Boric acid (HB) was sourced from Beijing InnoChem Science & Technology Co., Ltd., Hydroxylamine nitrate (HAN) was sourced from the Sixth Academy of China Aerospace Science and Technology Corporation with a content of 99.0%. All the aforementioned materials were utilized without additional purification. Distilled water was self-made.

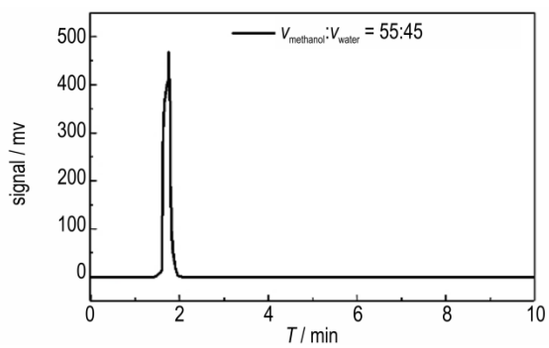

Fig.1 HPLC of NTO

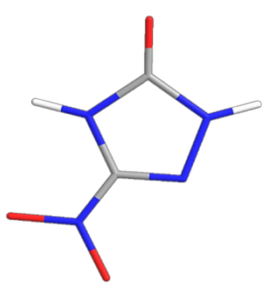

Fig.2 The molecular structure of NTO

1.2 Differential scanning calorimetry

Using the DSC 214 Polyma, the melting point (T_m) and enthalpy of fusion ($\Delta_{fus}H$) of 3-nitro-1, 2, 4-triazole-5-one (NTO) were analyzed. Prior to the measurements, the DSC instrument was calibrated with neat indium to ensure accuracy in temperature deviation, thermal deviation, and thermal repeatability. Approximately 5 mg of NTO was subjected to a heating rate of 10 K·min^{-1} and a nitrogen flow rate of 150 mL·min^{-1} for protection. The results indicated that the melting temperature and the fusion enthalpy of NTO are 543.35 K and 234.90 kJ·mol^{-1}, respectively, as presented in Fig.3.

1.3 X-ray diffraction

The crystal form of NTO recovered from the two systems was investigated using a Bruker D8 system to determine if dissolution altered its crystalline structure. The test tube voltage and current settings

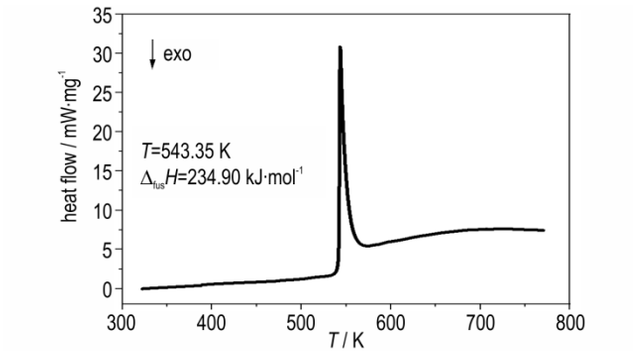

Fig.3 DSC curve of NTO

were 40 kV and 30 mA, respectively. The diffraction peaks were scanned over a range from 3° to 90° (2θ) at a scanning speed of 5°·min^{-1}. The analysis data confirmed that the crystal form of NTO remained unchanged by the components of the two systems, as illustrated in Fig.4.

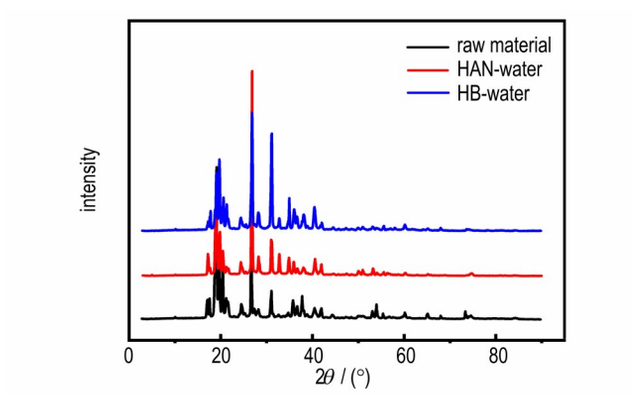

Fig.4 Powder X-ray diffraction patterns of NTO and NTO in two systems (HAN-water and HB-water)

1.4 Solubility measurements

The solubility of NTO in two different solvent systems was analyzed using a laser monitoring approach[8-9]. The experiments utilized a jacketed glass container equipped with a magnetic stirrer. The volume of the solution was measured with an accuracy of 0.1 mL using a pipette, and the mass of NTO was determined to an accuracy of 0.0001 g using an analytical balance (GP-300S, China). As NTO dissolved in the solvent system, the intensity of the laser beam penetrating the container progressively increased from a low initial value to its maximum at the point of complete dissolution. The volume of solvent at which maximum intensity was observed was recorded. To ensure the accuracy and reliability of the results, each experiment was conducted at least three times. The mole fraction solubility (x_1) of NTO was then calculated using the following formula:

$$x_1 = \frac{m_1/M_1}{m_1/M_1 + m_2/M_2 + m_3/M_3} \quad (1)$$

$$\omega_1 = \frac{m_2}{m_2 + m_3} \quad (2)$$

In this context, x_1 represents the solubility of NTO, ω_1 represents the proportion of water in the system, and m_1/M_1, m_2/M_2, and m_3/M_3 denote the mass-to-molecular weight ratios of NTO, water, and HAN or HB, respectively. The results of the correlation analysis using the modified Apelblat equation are depicted in Figs.5 and 6.

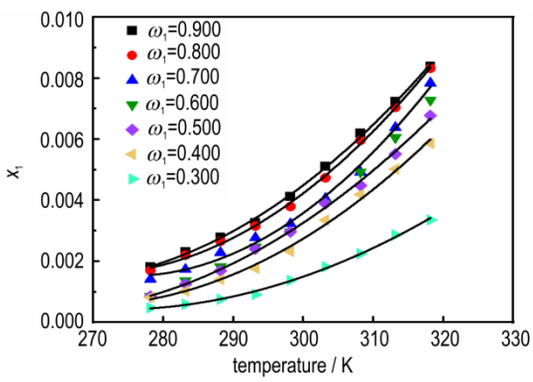

Fig. 5 Experimental data correlated by modified Apelblat equation in (HAN-water) binary solvent mixtures

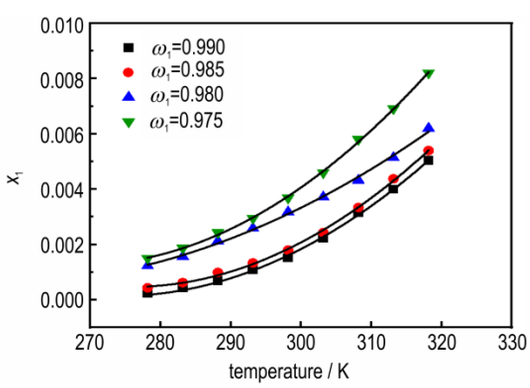

Fig. 6 Experimental data correlated by modified Apelblat equation in (HB-water) binary solvent mixtures

1.5 Solubility models

The root-mean-square deviation (RMSD) is obtained by Eq.(3).

$$\mathrm{RMSD} = \left[\frac{\sum_{i=1}^{n}\left(x^c - x^e\right)^2}{N}\right]^{1/2} \quad (3)$$

Where x^e and x^c are the experimental data and the

calculated values, respectively.

1.5.1 The modified Apelblat equation

The relationship between temperature and solubility was analyzed using the modified Apelblat equation[10-16]. The analysis revealed a straightforward correlation, generally expressed as following:

$$\ln x_1 = A + \frac{B}{T} + C\ln T \quad (4)$$

Where A, B, and C denote three empirical constants, the specific values of which are shown in Table 1, along with other model parameters of 10^5RMSD and R^2.

Table 1 Model parameters, 10^5RMSD and R^2 of the modified Apelblat equation in different binary solvents

system	ω_1	A	B	C	10^5 RMSD	R^2
HAN-water	0.900	309.0	-1.807×10^4	−44.76	8.584	0.9959
	0.800	198.3	-1.166×10^4	−28.95	8.713	0.9982
	0.700	99.6	-7.610×10^3	−13.96	7.878	0.9984
	0.600	−188.3	5.043×10^3	29.20	6.202	0.9979
	0.500	329.5	-1.927×10^4	−47.54	9.443	0.9972
	0.400	279.0	-1.649×10^4	−40.27	11.430	0.9991
	0.300	243.1	-1.510×10^4	−34.80	6.272	0.9988
HB-water	0.990	116.1	-8.687×10^3	−16.25	6.348	0.9991
	0.985	242.2	-1.393×10^4	−35.32	7.871	0.9960
	0.980	−74.7	-1.356×10^3	12.80	4.893	0.9986
	0.975	841.9	-4.347×10^4	−123.3	7.622	0.9981

1.5.2 Van't Hoff equation

The relationship can be further depicted using the Van't Hoff equation[17], as following:

$$\ln x_1 = A + \frac{B}{T} \quad (5)$$

Where A and B denote two model parameters, the specific values of which are shown in Table 2, along with model parameters of 10^5 RMSD and R^2.

1.5.3 λh equation

The λh equation proposed by Buchowski et al., can be expressed as below[18], which is used for the fitness of solubility data in most systems with two variables of λ and h.

$$\frac{1}{x_1} - 1 = \frac{1}{\lambda}\left\{\exp\left[\lambda h\left(\frac{1}{T} - \frac{1}{T_m}\right)\right] - 1\right\} \quad (6)$$

Where T_m denotes the melting point of NTO, and the specific values of the model parameters are shown in Table 3, including λ, h, 10^5 RMSD and R^2.

1.5.4 CNIBS/R-K model

The CNIBS/R-K equation[19-22] proposed by Acree et al., simulated the solubility of solutes in bi-

Table 2 Parameters of Van't Hoff equation for NTO in different binary solvents

system	ω_1	A	B	10^5 RMSD	R^2
HAN-water	0.900	5.892	−3389	9.692	0.9981
	0.800	6.404	−3558	8.904	0.9983
	0.700	7.506	−3936	13.22	0.9961
	0.600	8.473	−4256	10.97	0.9973
	0.500	7.864	−4086	14.25	0.9946
	0.400	8.477	−4321	16.69	0.9909
	0.300	8.323	−4450	6.264	0.9938
HB-water	0.990	7.100	−3782	7.146	0.9989
	0.985	5.444	−3349	4.733	0.9969
	0.980	11.330	−5260	8.290	0.9976
	0.975	12.680	−5709	13.70	0.9938

Table 3 Parameters of λh equation for NTO in different binary solvents

system	ω_1	λ	h	10^5 RMSD	R^2
HAN-water	0.900	1.817	1870	2.118	0.9980
	0.800	2.336	1527	2.514	0.9983
	0.700	3.930	1004	4.600	0.9960
	0.600	6.292	678.8	8.850	0.9974
	0.500	4.412	928.4	10.12	0.9947
	0.400	5.704	759.7	6.597	0.9910
	0.300	3.921	1136	6.250	0.9939
HB-water	0.990	3.334	1141	1.492	0.9990
	0.985	1.221	2744	4.725	0.9969
	0.980	22.830	231.0	8.010	0.9976
	0.975	47.060	122.6	25.11	0.9922

nary solvent systems, as following:

$$\ln x_1 = B_0 + B_1 x_2 + B_2 x_2^2 + B_3 x_2^3 + B_4 x_2^4 \quad (7)$$

Where B_0, B_1, B_2, B_3 and B_4 denote five model parameters, the specific values of which are shown in Table 4, along with other model parameters of 10^5 RMSD and R^2.

Table 4 Model parameters of the CNIBS/R-K model in different binary solvents

system	T / K	B_0	B_1	B_2	B_3	B_4	10^5RMSD	R^2
	278.15	−42.34	151.6	−247.1	176.3	−44.54	8.594	0.9417
	283.15	−46.74	147.9	−200.3	113.0	−19.73	18.01	0.9802
	288.15	−56.06	181.0	−240.2	132.7	−23.16	9.817	0.9843
	293.15	−55.02	145.6	−127.2	10.05	20.96	11.87	0.9901
HAN-water	298.15	−24.57	−3.87	156.7	−233.0	99.45	7.885	0.9886
	303.15	−70.20	193.2	−154.3	−18.97	45.24	10.83	0.9921
	308.15	−69.64	206.5	−204.3	40.31	22.17	15.25	0.9784
	313.15	−60.41	191.2	−228.3	100.9	−8.214	18.38	0.9921
	318.15	−50.32	154.4	−184.2	85.29	−9.837	20.23	0.9948
	278.15	−744.5	−34.18	660.2	1425	−1312	9.868	0.9056
	283.15	−2352	2391	1010	−58.42	−995.6	10.78	0.9149
	288.15	−1820	−1880	7219	−1717	−1807	15.34	0.9176
	293.15	−314.2	9.574	212.9	566.5	−479.9	13.65	0.9138
HB-water	298.15	−1849	190.2	3607	−550.3	−1403	16.02	0.9401
	303.15	692.7	−841.1	−223.8	−16.03	383.5	19.23	0.9654
	308.15	846.5	−1505	390.3	162.8	100.4	8.365	0.9588
	313.15	842.7	68.19	−682.6	−2410	2177	16.37	0.9646
	318.15	251.6	112.1	−235.6	−1025	893.0	20.28	0.9379

1.6 Apparent thermodynamic properties

According to the solubility data of NTO, the apparent thermodynamic properties (e.g., ΔH^{Θ}_{soln}, ΔS^{Θ}_{soln} and ΔG^{Θ}_{soln}) can be calculated, and based on Van't Hoff equation, ΔH^{Θ}_{soln} can be calculated[23]:

$$\Delta H^{o}_{soln} = -R \times \frac{\partial \ln x_1}{\partial (1/T)} = -R \times \frac{\partial \ln x_1}{\partial (1/T - 1/T_{hm})} = -R \times slope \quad (8)$$

Where T_{hm} denotes the mean harmonic temperature[24], which can be defined by the following Eq.(9), and the slope can be derived from Fig.7.

$$T_{hm} = \frac{n}{\sum_{i=1}^{n} \frac{1}{T_i}} \quad (9)$$

Where n denotes the number of temperatures; T_i is the experimental temperature; and the value of T_{hm} is 297.59 K.

The ΔG^{Θ}_{soln} is defined as below[25]:

$$\Delta G^{\Theta}_{soln} = -RT_{hm} \times intercept \quad (10)$$

Where intercept denotes the intercept of $\ln x_1 - (1/T - 1/T_{hm})$

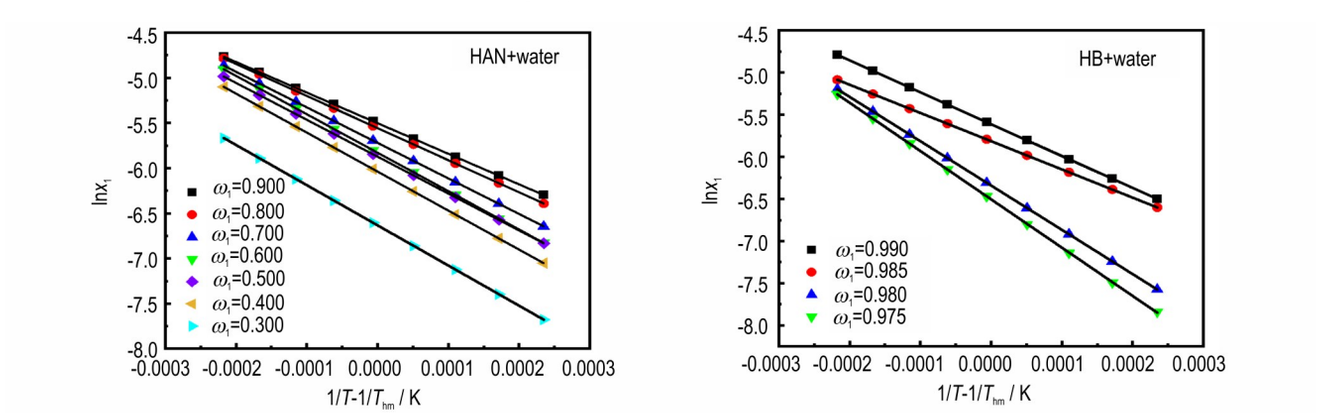

Fig.7 $\ln x_1$ of NTO in two binary solvents against $(1/T - 1/T_{hm})$

curve.

The ΔS^{Θ}_{soln} is described by Eq.(11).

$$\Delta S^{\Theta}_{soln} = \left(\Delta H^{\Theta}_{soln} - \Delta G^{\Theta}_{soln}\right)/T_{hm} \quad (11)$$

Following the calculations as per Equation (12) and Equation (13)[26-27], the relative contributions of enthalpy and entropy to the standard molar Gibbs free energy can be determined.

$$\%\zeta_H = \frac{|\Delta H^{\Theta}_{soln}|}{|\Delta H^{\Theta}_{soln}| + |T_{hm} \cdot \Delta S^{\Theta}_{soln}|} \times 100 \quad (12)$$

$$\%\zeta_{TS} = \frac{|T_{mean} \cdot \Delta S^{o}_{soln}|}{|\Delta H^{\Theta}_{soln}| + |T_{hm} \cdot \Delta S^{\Theta}_{soln}|} \times 100 \quad (13)$$

The apparent thermodynamic functions for the two binary systems following the dissolution of NTO are presented in Table 5.

Table 5 $\%\zeta_H$, $\%\zeta_{TS}$, ΔH^{Θ}_{soln}, ΔS^{Θ}_{soln} and ΔG^{Θ}_{soln} of NTO in two binary solvents at T_{hm}=297.59 K and P=0.1 MPa

system	ω_1	ΔH^{Θ}_{soln} /kJ·mol^{-1}	ΔS^{Θ}_{soln} /J·K^{-1}·mol^{-1}	ΔG^{Θ}_{soln} /kJ·mol^{-1}	$\%\zeta_H$	$\%\zeta_{TS}$
HAN-water	0.900	28.42	49.74	13.62	65.75	34.25
	0.800	29.10	51.63	13.74	65.45	34.55
	0.700	31.09	57.03	14.12	64.69	35.31
	0.600	38.09	79.33	14.48	61.74	38.26
	0.500	37.34	76.38	14.61	62.16	37.84
	0.400	38.03	77.37	15.00	62.29	37.71
	0.300	37.81	71.80	16.45	63.89	36.11
HB-water	0.990	31.67	59.72	13.89	64.05	35.95
	0.985	29.07	49.28	14.41	66.47	33.53
	0.980	46.67	103.8	15.77	60.16	39.84
	0.975	55.29	131.1	16.28	58.63	41.37

2 Results and discussion

In binary solvents, solubility is affected by many factors, such as temperature, van der Waals forces and hydrogen bonds. The solubility of NTO displays an upward trend with an increase in temperature, as illustrated in Figs 5-6. In the HB-water system, when the mass fraction of water (ω_1) decreased from 0.990 to 0.975, the relative content of water did not change much, so the influence of the amount of solvent on the solubility of NTO could be ignored. Therefore, the factors affecting the solubility of NTO are temperature and acidity of the system. The acidity of boric acid comes from the release of protons from hydroxide ions in bound water molecules, and H—O hydrogen bonds are more easily formed in this system. Thus, the solubility of NTO increases with the increase of HB concentration. On the contrary, in the HAN-water system, the solubility of NTO decreases with the increase of HAN content. There are three main reasons affecting the solubility of NTO in HAN-water system. Firstly, HAN is acidic, which inhibits the ionization of NTO; secondly, with the increase of HAN content, the content of water decreases, so the solubility decreases; thirdly, the polarity of HAN is much greater than that of NTO, and water is more inclined to form a hydrogen spectrum with HAN, so the interaction with NTO is weakened, and thus the solubility is reduced.

The solubility of a solute generally depends on its molecular similarities to the solvents. As Mullin[28] describes, in polar solvents, the interaction between solvent molecules is predominantly governed by the formation of robust hydrogen bonds, which could be disrupted by the solute and replaced with equivalently strong bonds during the dissolution process. As shown in Fig. 2, NTO, characterized by its five-membered ring structure, features electron-withdrawing —NO_2 groups, which would reduce the electron density around the nitrogen atoms. These enables NTO to act as hydrogen bond donor, which facilitates the formation of hydrogen bonds with solvent molecules. Consequently, solubility is influenced by both van der Waals forces, indicative of polarity, and hydrogen bonding dynamics, which govern the solute-solvent interaction[29]. Therefore, an increase in the water content in the HB-water systems weakens the interaction between NTO and organic solvents, leading to decreased solubility at a given temperature. While polarity primarily affects the strength of van der Waals interactions, hydrogen bonding often plays a crucial role in solute-solvent dynamics. This phenomenon is similar to those observed in other compounds, such as EA[30], CNP[31], and formaldehyde (FM)[32].

Tables 1-4 clearly demonstrate that the average 10^5RMSD values for the solubility models are as follows: 7.55 for the modified Apelblat equation, 10.35 for the Van't Hoff equation, 7.31 for the λh equation, and 13.93 for the CNIBS/R-K equation. The corresponding average R^2 are 0.9979, 0.9960, 0.9959, and 0.9589, respectively. These values indicate that all four equations provide satisfactory fits to the experimental data for NTO in mixed solvents, demonstrating strong correlations. Comparable to the data for RMSD and R^2, the modified Apelblat equation is shown to have the most precise correlation between solubility and temperature, followed by the λh equation, Van't Hoff equation, and CNIBS/R-K equation. This hierarchy reflects that the modified Apelblat equation is particularly effective for equation research, solvent selection, and accurately fitting the solubility values of NTO in binary systems compared to the other models. The results provide solid foundation for future research into the crystallization process of NTO.

The values of ΔH_{soln}^{Θ}, as shown in Table 5, are positive, suggesting that the dissolution of NTO is an endothermic process. The values of ΔS_{soln}^{Θ} are also positive, indicating that the entropy is entropy-driven. Moreover, all the values of ΔG_{soln}^{Θ} are positive, suggesting that the dissolution of NTO in the two systems is a non-spontaneous process. The $\%\zeta_H$ is larger than $\%\zeta_{TS}$, and all the $\%\zeta_H$ data are ⩾ 58.63%, indicating that the enthalpy make a greater contribution than entropy to the ΔG_{soln}^{Θ}.

3 Conclusions

In the study of using NTO to improve the energy characteristics of electronically controlled solid propellant, we need to clarify the solubility of NTO in the propellant system in order to obtain high quality propellant samples. According to the preparation process, the factors affecting the solubility of NTO in the system were determined as the contents of HAN, HB and water, and the solubility of NTO in the two binary solvents systems of HAN-water and HB-water was determined by dynamic laser monitoring method at the temperature of 278.15−318.15 K. The following conclusions are drawn:

1) The solubility of NTO in the two binary solvent systems is positively correlated with temperature, and the solubility increases with the increase of temperature. In the HAN-water system, the solubility is positively correlated with the mass fraction of water, and the solubility increases with the increase of the mass fraction of water; on the contrary, in the HB - water system, the solubility is negatively correlated with the mass fraction of water, and the solubility decreases with the increase of the mass fraction of water.

2) Comparing the effects of HAN and HB on the dissolution behavior of NTO in water, within the reasonable range of HB addition (1.0%−2.5%), HB promotes the dissolution of NTO, and at the same temperature, the more HB content there is, the greater the solubility of NTO; however, within the reasonable addition range of HAN (10%−70%), HAN inhibits the dissolution of NTO, and at the same temperature, the higher the HAN content, the lower the solubility of NTO.

3) X-ray diffraction results prove that NTO does not react with oxidant HAN and curing agent HB during the experiment, so NTO has good compatibility with the system. This results validates the operational safety of adding NTO to electronically controlled solid propellant systems.

4) The modified Apelblat model, Van't Hoff model, λh equation and CNIBS/R-K equations are suitable for correlating the measured solubility data and the calculated values were in agreement with the experimental data, and the R^2 of all four models exceeded 0.9. Among them, the 10^5RMSD of the modified Apelblat equation is the closest, both less than 11.43, and the mean value of 10^5RMSD is also small, which is the best match with the measured data. Therefore, in the subsequent formulation optimization, when changing the content of HAN, HB, water, and adjusting the curing temperature, the amount of NTO added under the current process pa-

rameters can be obtained by fitting and calculating according to the modified Apelblat equation.

5) Furthermore, the apparent thermodynamic properties, including ΔH_{soln}^{Θ}, ΔS_{soln}^{Θ} and ΔG_{soln}^{Θ}, were calculated by the Van't Hoff equation and Gibbs equations. It can be seen that the dissolution process of NTO is non-spontaneous, entropy-driven, and endothermic. In addition, the $\%\zeta_H$ is larger than $\%\zeta_{TS}$, and all the $\%\zeta_H$ data are ≥58.63%, indicating that the enthalpy make a greater contribution than entropy to the ΔG_{soln}^{Θ}.

References:

[1] WANG Zhi-wen, XIE Hai-ming, XIANG Shu-jie, et al. Multi-stage combustion characteristics of sodium perchlorate/lithium perchlorate-based electrically controlled solid propellant [J]. *Chemical Engineering Journal*, 2023, 456(2): 140958.

[2] LV Jia-rong, Research on the crystallization characteristics of NTO[D]. Taiyuan: North university of China, 2023.

[3] LI Xue, YI Zhi-wen, LIU Qiang, et al. Research of detonation products of RDX/Al from the perspective of composition [J]. *Defence Technology*, 2023, 24(6): 31−45.

[4] DING Kun, WANG Xue-yi, DUAN Zi, et al. Shock response of cyclotetramethylene tetranitramine (HMX) single crystal at elevated temperatures [J]. *Defence Technology*, 2023, 21(3): 147−163.

[5] LI Ming, HU Rui-rui, XU Ming, et al. Burning characteristics of high density foamed GAP/CL-20 propellants [J]. *Defence Technology*, 2022, 18(10): 1914−1921.

[6] LIN Lin, Wang Jian, Li Jing, et al. Symmetry breaking density functional theory study on the thermal decomposition mechanism of 3-nitro-1,2,4-triazole-5-one (NTO)[J]. *Chinese Journal of Organic Chemistry*, 2023,43(1): 285−294.

[7] LI Hong-zhen, HUANG Ming, LI Jin-shan, et al. Synthesis and crystal structure of 3-nitro-1,2,4-triazole-5-ketohydroxylamine salts[J]. *Chinese Journal of Synthetic Chemistry*, 2007, 1(6): 714−718.

[8] LAN Guan-chao, WANG Jian-long, CHEN Li-zhen, et al. Measurement and correlation of the solubility of 3,4-bis(3-nitrofurazan-4-yl)furoxan (DNTF) in different solvents[J]. *Journal of Chemical Thermodynamics*, 2015, 89(234): 264−269.

[9] LIU Yang, LI Yong-xiang, LAN Guan-chao, et al. Determination and correlation of solubility of 3,4-dinitro-1*H*-pyrazole in different pure solvents from 298.15 K to 338.15 K[J]. *Journal of Chemical&Engineering Data*, 2016, 61(3): 2516−2524.

[10] Apelblat A, Manzurola E, Solubility of o-acetylsalicylic, 4-aminosalicylic, 3,5-dinitrosalicylic, and p-toluic acid and magnesium-DL-aspartate in water from *T*=(278 to 348) K[J]. *Journal of Chemical Thermodynamics*, 1998, 31(9): 85−91.

[11] CHENG Yi, SHAO Ying-yi, YAN Wang, et al. Solubility of betulinic acid in thirteen organic solvents at different temperatures [J]. *Journal of Chemical&Engineering Data*, 2011, 56(13): 4587−4591.

[12] APELBLAT A, MANZUROLA E, Solubility of L-aspartic, DL-aspartic, DL-glutamic, p-hydroxybenzoic, o-anisic, p-anisic, and itaconic acids in water from *T*=278 K to *T*=345 K[J]. *Journal of Chemical Thermodynamics*,1997,29(20): 1527−1533.

[13] SUN Hua, LI Ming, JIA Jin-tian, et al. Measurement and correlation of the solubility of 2,6-disaminohexanoic acid hydrochloride in aqueous methanol and aqueous ethanol mixtures [J]. *Journal of Chemical & Engineering Data*, 2012, 5(5): 1463−1467.

[14] LI Rong-rong, YING An-guo, HUANG Guo-bo, et al. Equilibrium solubility of sodium 3-sulfobenzoate in binary(sodium chloride+water), (sodium sulfate+water), and (ethanol+water) solvent mixtures at temperatures from (278.15 to 323.15) K[J]. *Journal of Chemical Thermodynamics*, 2014, 79(11): 8−11.

[15] BUSTAMANTE P, ROMERO S, REILLO A, et al. Thermodynamics of paracetamol in amphiprotic and amphiprotic-aprotic solvent mixtures[J]. *Pharmaceutical Sciences*, 1995, 1(15): 505−507.

[16] DELGADO R, PENA M A, MARTINEZ F, et al. Preferential solvation of some sulfonamides in propylene glycol+water solvent according to the KIBI and QLQC methods[J]. *Journal of Solution Chemistry*, 2014, 43(4): 360−374.

[17] SCHRÖDER B, SANTOS L, MARRUCHO I M, et al. Prediction of aqueous solubilities of solid carboxylic acids with COSMO-RS [J]. *Fluid Phase Equilibria*, 2010, 289(4): 140−147.

[18] BUCHOWSKI H, KHIAT A, Solubility of solids in liquids: one-parameter solubility equation [J]. *Fluid Phase Equilibria*, 1986, 25(1): 273−278.

[19] LIU Cheng, TANG Gui-wen, DING Hui, et al. Determination of the solubility and thermodynamic properties of wedelolactone in a binary solvent of ethanol and water[J]. *Fluid Phase Equilibria*, 2015, 385(12): 139−146.

[20] YU Jin, MA Tian-lu, CHEN Xu, et al. Solubility of disodium cytidine 5′-monophosphate in different binary mixtures from 288.15 K to 313.15 K[J]. *Thermochima Acta*, 2013, 565(7): 1−7.

[21] ACREE J W E, Mathematical representation of thermodynamic properties: Part 2. Derivation of the combined nearly ideal binary solvent (NIBS)/Redlich-Kister mathematical representation from a two-body and three-body interactional mixing model[J]. *Thermochima Acta*, 1992, 198(10): 71−79.

[22] JOUYBAN G A, ACREE J W E. Comparison of models for describing multiple peaks in solubility profiles [J]. *International Journal of Pharmaceutics*, 1998, 167(05): 177−182.

[23] SHAKEEL F, HAQ N, EL-BADRY M, Thermodynamics and solubility of tadalafil in diethylene glycol monoethyl ether + water co-solvent mixtures at (298.15 to 333.15) K[J]. *Journal of Molecular Liquids*, 2014, 197(13): 334−338.

[24] ZHANG Fang, TANG Yao-cun, WANG Long, et al. Solubility measurement and correlation for 2-naphthaldehyde in pure organic solvents and methanol + ethanol mixtures[J]. *Journal of Chemical & Engineering Data*, 2015, 60(32): 2502−2509.

[25] KSIAZCZAK A, MOORTHI K, NAGATA I, et al. Solid-solid

transition and solubility of even *n*-alkanes[J]. *Fluid Phase Equilibria*, 1994, 95(18): 15-29.

[26] PERLOVICH G L, KURKOV S V, BAUER-BRANDL A, et al. Thermodynamics of solutions. II. Flurbiprofen and diflunisal as models for studying solvation of drug substances[J]. *European Journal of Pharmaceutical Sciences*, 2003, 19(4): 423-432.

[27] PERLOVICH G L, KURKOV S V, KINCHIN A N, et al. Thermodynamics of solutions III: comparison of the solvation of (+)-naproxen with other NSAIDs[J], *European Journal of Pharmacology*, 2004, 57(32): 411-420.

[28] MULLIN J W. Crystallization, butterworth-Heinemann[S], Oxford, 2001.

[29] WU Kun, LI Yi-jian, et al. Solubility and solution thermodynamics of p-toluenesulfonamide in 16 solvents from *T*=273.15 K to 324.75 K[J]. *Journal of molecular liquids*, 2019, 294: 111577.

[30] TONG Yao, WANG Zi-zi, YANG Eng-ti, et al. Determination and correlation of solubility and solution thermodynamics of ethenzamide in different pure solvents[J]. *Fluid Phase Equili*, 2016, 427(2): 549-556.

[31] ZHANG Rui, FENG Zi-jian, JI Jian-bin, et al. Measurement and correlation of solubility of two isomers of cyanopyridine in eight pure solvents from 268.15 K to 318.15 K[J]. *J Chem Eng Data*, 2017, 62(23): 3241-3251.

[32] QIN Yu-zi, WANG Hong-shan, YANG Peng, et al. Measurement and correlation of solubility and dissolution properties of flunixin meglumine in pure and binary solvents[J]. *Fluid Phase Equilibria*, 2015, 403(11): 145-152.

3-硝基-1,2,4-三唑-5-酮(NTO)在不同二元溶剂中的溶解度和热力学模型

郭昊琪,杨玉林

(哈尔滨工业大学化学与化工学院空间电源国家重点实验室, 黑龙江 哈尔滨 150001)

摘 要: 在278.15K~318.15K的温度范围内,利用动态激光监测法测定了3-硝基-1,2,4-三唑-5-酮(NTO)在硝酸羟胺(HAN)-水和硼酸(HB)-水两种不同二元体系中的溶解度。实验数据表明,NTO在二元溶剂混合物中的溶解度与温度呈正相关。此外,用修正的Apelblat方程、Van't-Hoff方程、λh方程和CNIBS/R-K方程对溶解度数据进行了拟合,所有模型在二元溶剂中都取得了令人满意的结果。本文计算的均方根偏差的平均值(10^5RMSD)均小于13.93。最后,用Van't-Hoff和Gibbs方程计算了表观热力学性质,即吉布斯能、焓和熵。本文计算的%ζ_H大于%ζ_{TS},且%ζ_H均≥58.63%,表明焓对吉布斯能的贡献大于熵。

关键词: 3-硝基-1,2,4-三唑-5-酮;溶解度;热力学模型;表观热力学分析

中图分类号: TJ55;O64 **文献标志码:** A **DOI:**10.11943/CJEM2024184

(责编:高 毅)